

Supplementary Material for Impact of Regional Marine Cloud Brightening Interventions on Climate Tipping Points

Section S1. Climate tipping point calculation

We assess the MCB impact on tipping points by computing the change in selected tipping point metrics (TPMs) in our CESM2 simulations (Table S1), based on supplementary discussion from a recent synthesis paper (McKay et al., 2022). These TPMs are not direct measures of tipping point risk. However, they are proximal indicators of the tendency of climate change impacts on each tipping point. We note that some of the tipping points considered herein are not possible in CESM2 due to missing process representation (such as icesheet height changes). Furthermore, CESM2 has substantial biases in key fields related to each tipping point, which likely introduces errors in each, compounding with uncertainties in the large scale climate response.

Arctic (a) and Barents (b) winter sea ice

We compute the Arctic (60N to 90N) and Barents (70N to 80N; 10E to 60E) Sea March April sea ice area (the winter sea ice maximum), which may rapidly transition into a year-round ice free state under sufficient warming (Drijfhout et al., 2015; Eisenman & Wettlaufer, 2009). Though Arctic winter sea ice collapse is very unlikely under SSP2-4.5 warming, regional winter sea ice collapse may occur in regions like the Barents Sea (McKay et al., 2022). However, we do not see winter sea ice collapse either region in CESM2 (Fig. S2). Furthermore, CESM2 generally underestimates present day Arctic sea ice extent (Danabasoglu et al., 2020), which may indicate sea ice may be too sensitive to warming in the model (Kay et al., 2021; Massonnet et al., 2018).

Greenland warming (c)

We compute annual mean 2-metre temperature over Greenland (60N to 80N; 60W to 20W) to assess the possible MCB impact on the elevation feedback, wherein icesheet thinning due to melt causes additional warming and further melt (Crowley & Baum, 1995; Robinson et al., 2012). However, we do not use a CESM2 configuration with two-way coupling between the Greenland ice sheet and atmosphere. Thus, the elevation feedback does not operate in our simulations and the temperature changes in the model may be underestimated.

Atlantic Meridional Overturning (d) and North Atlantic Gyre (e)

We compute the Annual mean AMOC index (Cheng et al., 2013) as a measure of overturning strength and North Atlantic (45N to 60N; 50W to 20W) area-mean annual maximum mixed layer depth as a measure of ocean convection strength (Swingedouw et al., 2021). These are two related tipping points associated with Atlantic Ocean circulation. CESM2 overestimates

present day AMOC strength by 2-3 Sv (Danabasoglu et al., 2020) and experiences a rapid, but linear decline in AMOC index over the SSP2-4.5 simulation (Fig. S2). CESM2 has lower North Atlantic subpolar gyre stratification than observed (Swingedouw et al., 2021), and thus may have a too-sensitive convection response.

North American (f) and Eurasian (g) permafrost area

We compute the areal extent of North American (60N to 75N; 160W to 60W) and Eurasian (60N to 80N; 65E to 180E) boreal permafrost, defined as land model grid points where the annual minimum soil ice concentration > 0 at 3.5m for the present and prior year. This is the definition of (Slater & Lawrence, 2013), except we use the land model's soil ice concentration rather than soil temperature $< 0^{\circ}\text{C}$, though this has little effect in the resulting permafrost area. Abrupt regional permafrost thaw is hypothesized to be a result of localized feedback processes (Schuur et al., 2015), which may occur across a region in a short period of time. However, such processes are difficult to represent on ESM spatial scales (Lawrence et al., 2019) and CESM2 projects substantial but linear losses in permafrost area under SSP2-4.5.

Amazon water deficit (h) and Sahel rainfall (i)

CESM2 does not include dynamic vegetation biogeography (Lawrence et al., 2019). Thus, we cannot directly assess vegetation change in the model. In the case of the Amazon, we therefore estimate MCB effect of possible Amazon rainforest dieback using the area-mean (7S to 7S; 70W to 45W) maximum climatological water deficit (MCWD) defined as the most negative value of the cumulative precipitation minus evaporation over a year (Malhi et al., 2009). MCWD and annual precipitation together can be used to classify vegetation type in the Amazon (Malhi et al., 2009), and changes in the hydroclimate could trigger dieback of the rainforest. Additionally, CESM2 has a substantial dry bias in the Amazon (Danabasoglu et al., 2020), which introduces uncertainty in the precipitation response to forcing in the region.

In the case of the Sahel (10N to 20N; 15W to 35E), we simply assess the regional mean, annual mean precipitation, which is an indicator of West African monsoon strength. It is thought that vegetation-albedo feedback could rapidly increase monsoon strength and vegetation cover in the region, as occurred in the Green Sahara period (Hopcroft & Valdes, 2021; Pausata et al., 2020). There is substantial inter-model uncertainty regarding the greenhouse gas impact on the Sahel (Monerie et al., 2020). Though we consider Sahel greening a risk of GHG/MCB forcing here, some have argued for geoengineering via large-scale afforestation wherein greening is considered desirable (Pausata et al., 2020).

Amundsen sea zonal wind speed (j)

For West Antarctic icesheet collapse, we assume marine ice sheet instability due to grounding lines reaching retrograde slopes is the principle tipping point (e.g., Feldmann & Levermann, 2015). Marine ice sheet melt is principally driven by circumpolar deep water flow into the vicinity of the ice sheets (Jenkins et al., 2018), which is correlated with wind stress and zonal wind speed in the Amundsen sea off the coast of West Antarctica (Holland et al., 2019). Thus, we use Pine Island/Thwaites Troughs (71.8S to 70.2S; 115W to 102W) area-mean annual mean zonal wind speed to estimate the GHG/MCB effect on West Antarctic ice sheet melt (Holland et

al., 2019). Our CESM2 experiments do not include two-way coupling to ice sheet dynamics; thus, we cannot directly assess ice sheet changes. Furthermore, the averaging box is derived from observational conditions, and thus may not be suitable for CESM2, which is coarser resolution and has different sea ice distribution in the region compared to observed.

Coral heat stress (k, l, m, n)

We consider the impact of GHG/MCB forcing on coral reefs in four regions (Caribbean Sea - 12N to 25N; 85W to 65W, West Indian Ocean - 25S to 0; 35E to 60E, West Tropical Pacific Ocean - 10S to 10N; 100E to 150E, Coral Sea - 25S to 10S; 145E to 165E) by computing changes in the area-mean annual maximum degree heating weeks (DHW) (Liu et al., 2003). DHW is the cumulative weekly anomaly above a threshold equal to maximum monthly mean temperature over a reference period (1990-1999) of historical CESM2 plus 1C in a twelve-week window. Severe heat stress is considered to occur if $DHW > 8$ C-weeks (Latham et al., 2013; Liu et al., 2003). Here we simply assess the change in annual maximum DHW as a measure of the mean intensity of summertime hot conditions in a region.

Table S1. Summary of climate tipping point metrics assessed in Fig. 3

Fig. 3 Label	Tipping Point	Metric	Citation
a	Arctic winter sea ice	March-April sea ice area (60N to 90N)	(Drijfhout et al., 2015)
b	Barents Sea winter sea ice	March-April sea ice area (70N to 80N; 10E to 60E)	(Drijfhout et al., 2015)
c	Greenland icesheet	Annual mean 2m temperature (land; 60N to 80N; 60W to 20W)	(Crowley & Baum, 1995; Robinson et al., 2012)
d	Atlantic Meridional Overturning	Annual mean Atlantic meridional streamfunction maximum at 30N	(Cheng et al., 2013; Swingedouw et al., 2021)
e	North Atlantic Gyre	Annual maximum mixed layer depth (ocean; 45N to 60N; 50W to 20W)	(Sgubin et al., 2017; Swingedouw et al., 2021)
f	North American Permafrost	Land area where annual minimum soil ice concentration > 0 at 3.5m for two consecutive years (land; 60N to 75N; 160W to 60W)	(Lawrence et al., 2012; Slater & Lawrence, 2013)
g	Eurasian Permafrost	Land area where annual minimum soil ice concentration > 0 at 3.5m for two consecutive years (land; 60N to 80N; 65E to 180E)	(Lawrence et al., 2012; Slater & Lawrence, 2013)
h	Amazon water deficit	Annual maximum water deficit (land; 7S to 7S; 70W to 45W)	(Malhi et al., 2009)

i	Sahel rainfall	Annual mean precipitation (land; 10N to 20N; 15W to 35E)	(Hopcroft & Valdes, 2021; Pausata et al., 2020)
j	Amundsen sea windspeed	Annual mean Amundsen sea surface zonal wind speed (ocean; 71.8S to 70.2S; 115W to 102W)	(Holland et al., 2019)
k	Caribbean Sea coral heat stress	Annual maximum degree heating weeks (ocean; 12N to 25N; 85W to 65W)	(Liu et al., 2003)
l	West Indian Ocean coral heat stress	Annual maximum degree heating weeks (ocean; 25S to 0; 35E to 60E)	(Liu et al., 2003)
m	West Tropical Pacific coral heat stress	Annual maximum degree heating weeks (ocean; 10S to 10N; 100E to 150E)	(Liu et al., 2003)
n	Coral Sea coral heat stress	Annual maximum degree heating weeks (ocean; 25S to 10S; 145E to 165E)	(Liu et al., 2003)

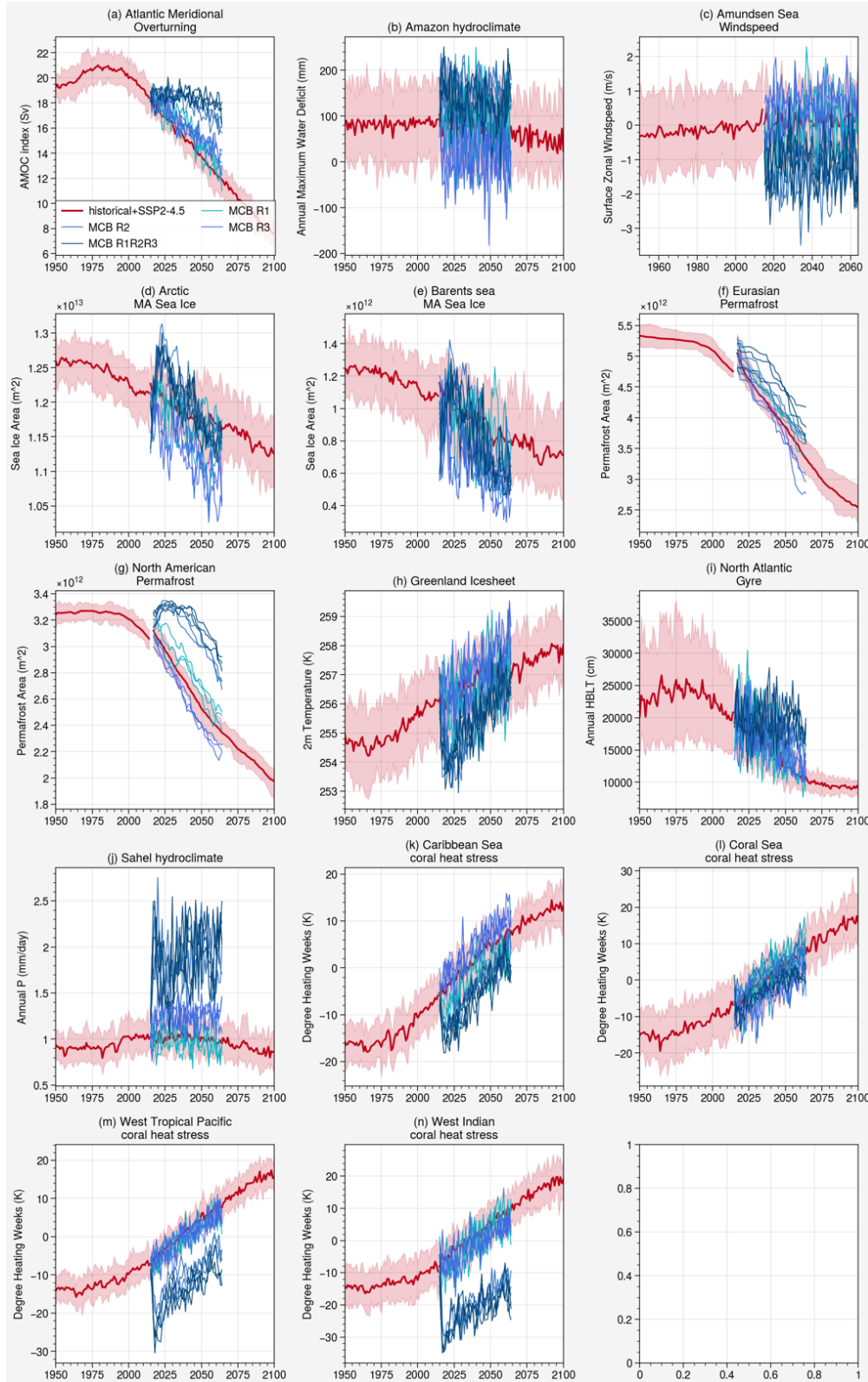


Fig. S1. Time series of Tipping point metric changes for historical and SSP2-4.5 (red) and the SSP2-4.5 + MCB simulations (blue shades). Solid red line indicates ensemble average and red shading indicates 5 to 95 percentile range.

- Cheng, W., Chiang, J. C. H., & Zhang, D. (2013). Atlantic Meridional Overturning Circulation (AMOC) in CMIP5 Models: RCP and Historical Simulations. *Journal of Climate*, 26(18), 7187–7197. <https://doi.org/10.1175/JCLI-D-12-00496.1>
- Crowley, T. J., & Baum, S. K. (1995). Is the Greenland Ice Sheet bistable? *Paleoceanography*, 10(3), 357–363. <https://doi.org/10.1029/95PA00662>
- Danabasoglu, G., Lamarque, J. -F., Bacmeister, J., Bailey, D. A., DuVivier, A. K., Edwards, J., Emmons, L. K., Fasullo, J., Garcia, R., Gettelman, A., Hannay, C., Holland, M. M., Large, W. G., Lauritzen, P. H., Lawrence, D. M., Lenaerts, J. T. M., Lindsay, K., Lipscomb, W. H., Mills, M. J., ... Strand, W. G. (2020). The Community Earth System Model Version 2 (CESM2). *Journal of Advances in Modeling Earth Systems*, 12(2). <https://doi.org/10.1029/2019MS001916>
- Drijfhout, S., Bathiany, S., Beaulieu, C., Brovkin, V., Claussen, M., Huntingford, C., Scheffer, M., Sgubin, G., & Swingedouw, D. (2015). Catalogue of abrupt shifts in Intergovernmental Panel on Climate Change climate models. *Proceedings of the National Academy of Sciences*, 112(43). <https://doi.org/10.1073/pnas.1511451112>
- Eisenman, I., & Wettlaufer, J. S. (2009). Nonlinear threshold behavior during the loss of Arctic sea ice. *Proceedings of the National Academy of Sciences*, 106(1), 28–32. <https://doi.org/10.1073/pnas.0806887106>
- Feldmann, J., & Levermann, A. (2015). Collapse of the West Antarctic Ice Sheet after local destabilization of the Amundsen Basin. *Proceedings of the National Academy of Sciences*, 112(46), 14191–14196. <https://doi.org/10.1073/pnas.1512482112>

- Holland, P. R., Bracegirdle, T. J., Dutrieux, P., Jenkins, A., & Steig, E. J. (2019). West Antarctic ice loss influenced by internal climate variability and anthropogenic forcing. *Nature Geoscience*, 12(9), 718–724. <https://doi.org/10.1038/s41561-019-0420-9>
- Hopcroft, P. O., & Valdes, P. J. (2021). Paleoclimate-conditioning reveals a North Africa land–atmosphere tipping point. *Proceedings of the National Academy of Sciences*, 118(45), e2108783118. <https://doi.org/10.1073/pnas.2108783118>
- Jenkins, A., Shoosmith, D., Dutrieux, P., Jacobs, S., Kim, T. W., Lee, S. H., Ha, H. K., & Stammerjohn, S. (2018). West Antarctic Ice Sheet retreat in the Amundsen Sea driven by decadal oceanic variability. *Nature Geoscience*, 11(10), 733–738. <https://doi.org/10.1038/s41561-018-0207-4>
- Kay, J. E., DeRepentigny, P., Holland, M. M., Bailey, D. A., DuVivier, A. K., Blanchard-Wrigglesworth, E., Deser, C., Jahn, A., Singh, H. A., Smith, M. M., Webster, M. A., Edwards, J., Lee, S.-S., Rodgers, K., & Rosenbloom, N. A. (2021). *Less surface sea ice melt in the CESM2 improves Arctic sea ice simulation with minimal non-polar climate impacts* [Preprint]. *Climatology (Global Change)*. <https://doi.org/10.1002/essoar.10507477.1>
- Latham, J., Kleypas, J., Hauser, R., Parkes, B., & Gadian, A. (2013). Can marine cloud brightening reduce coral bleaching?: Can marine cloud brightening reduce coral bleaching? *Atmospheric Science Letters*, 14(4), 214–219. <https://doi.org/10.1002/asl2.442>
- Lawrence, D. M., Fisher, R. A., Koven, C. D., Oleson, K. W., Swenson, S. C., Bonan, G., Collier, N., Ghimire, B., van Kampenhout, L., Kennedy, D., Kluzek, E., Lawrence, P. J., Li, F., Li, H., Lombardozzi, D., Riley, W. J., Sacks, W. J., Shi, M., Vertenstein, M., ... Zeng, X. (2019). The Community Land Model Version 5: Description of New Features, Benchmarking, and

- Impact of Forcing Uncertainty. *Journal of Advances in Modeling Earth Systems*, 11(12), 4245–4287. <https://doi.org/10.1029/2018MS001583>
- Lawrence, D. M., Slater, A. G., & Swenson, S. C. (2012). Simulation of Present-Day and Future Permafrost and Seasonally Frozen Ground Conditions in CCSM4. *Journal of Climate*, 25(7), 2207–2225. <https://doi.org/10.1175/JCLI-D-11-00334.1>
- Liu, G., Strong, A. E., & Skirving, W. (2003). Remote sensing of sea surface temperatures during 2002 Barrier Reef coral bleaching. *Eos, Transactions American Geophysical Union*, 84(15), 137–141. <https://doi.org/10.1029/2003EO150001>
- Malhi, Y., Aragão, L. E. O. C., Galbraith, D., Huntingford, C., Fisher, R., Zelazowski, P., Sitch, S., McSweeney, C., & Meir, P. (2009). Exploring the likelihood and mechanism of a climate-change-induced dieback of the Amazon rainforest. *Proceedings of the National Academy of Sciences*, 106(49), 20610–20615. <https://doi.org/10.1073/pnas.0804619106>
- Massonnet, F., Vancoppenolle, M., Goosse, H., Docquier, D., Fichefet, T., & Blanchard-Wrigglesworth, E. (2018). Arctic sea-ice change tied to its mean state through thermodynamic processes. *Nature Climate Change*, 8(7), 599–603. <https://doi.org/10.1038/s41558-018-0204-z>
- McKay, D. I. A., Staal, A., Abrams, J. F., Winkelmann, R., Sakschewski, B., Loriani, S., Fetzer, I., Cornell, S. E., Rockström, J., & Lenton, T. M. (2022). Exceeding 1.5°C global warming could trigger multiple climate tipping points. *Science*, 377, 6611. <https://doi.org/10.1126/science.abn7950>
- Monerie, P.-A., Wainwright, C. M., Sidibe, M., & Akinsanola, A. A. (2020). Model uncertainties in climate change impacts on Sahel precipitation in ensembles of CMIP5 and CMIP6

simulations. *Climate Dynamics*, 55(5–6), 1385–1401. <https://doi.org/10.1007/s00382-020-05332-0>

Pausata, F. S. R., Gaetani, M., Messori, G., Berg, A., Maia de Souza, D., Sage, R. F., & deMenocal, P. B. (2020). The Greening of the Sahara: Past Changes and Future Implications. *One Earth*, 2(3), 235–250. <https://doi.org/10.1016/j.oneear.2020.03.002>

Robinson, A., Calov, R., & Ganopolski, A. (2012). Multistability and critical thresholds of the Greenland ice sheet. *Nature Climate Change*, 2(6), 429–432. <https://doi.org/10.1038/nclimate1449>

Schuur, E. A. G., McGuire, A. D., Schädel, C., Grosse, G., Harden, J. W., Hayes, D. J., Hugelius, G., Koven, C. D., Kuhry, P., Lawrence, D. M., Natali, S. M., Olefeldt, D., Romanovsky, V. E., Schaefer, K., Turetsky, M. R., Treat, C. C., & Vonk, J. E. (2015). Climate change and the permafrost carbon feedback. *Nature*, 520(7546), 171–179. <https://doi.org/10.1038/nature14338>

Sgubin, G., Swingedouw, D., Drijfhout, S., Mary, Y., & Bennabi, A. (2017). Abrupt cooling over the North Atlantic in modern climate models. *Nature Communications*, 8(1), 14375. <https://doi.org/10.1038/ncomms14375>

Slater, A. G., & Lawrence, D. M. (2013). Diagnosing Present and Future Permafrost from Climate Models. *Journal of Climate*, 26(15), 5608–5623. <https://doi.org/10.1175/JCLI-D-12-00341.1>

Swingedouw, D., Bily, A., Esquerdo, C., Borchert, L. F., Sgubin, G., Mignot, J., & Menary, M. (2021). On the risk of abrupt changes in the North Atlantic subpolar gyre in CMIP6

models. *Annals of the New York Academy of Sciences*, 1504(1), 187–201.

<https://doi.org/10.1111/nyas.14659>